Functional CD169 on Macrophages Mediates Interaction with Dendritic Cells for CD8+ T Cell Cross-Priming

van Dinther, Dieke; Veninga, Henrike; Iborra, Salvador; Borg, Ellen G. F.; Hoogterp, Leoni; Olesek, Katarzyna; Beijer, Marieke R.; Schetters, Sjoerd T. T.; Kalay, Hakan; Garcia-Vallejo, Juan J.; Franken, Kees L.; Cham, Lamin B.; Lang, Karl S.; van Kooyk, Yvette; Sancho, David; Crocker, Paul R.; den Haan, Joke M. M.

Published in:
Cell Reports

DOI:
10.1016/j.celrep.2018.01.021

Publication date:
2018

Document Version
Publisher's PDF, also known as Version of record

Article

Cell Reports

Functional CD169 on Macrophages Mediates Interaction with Dendritic Cells for CD8$^+$ T Cell Cross-Priming

Graphical Abstract

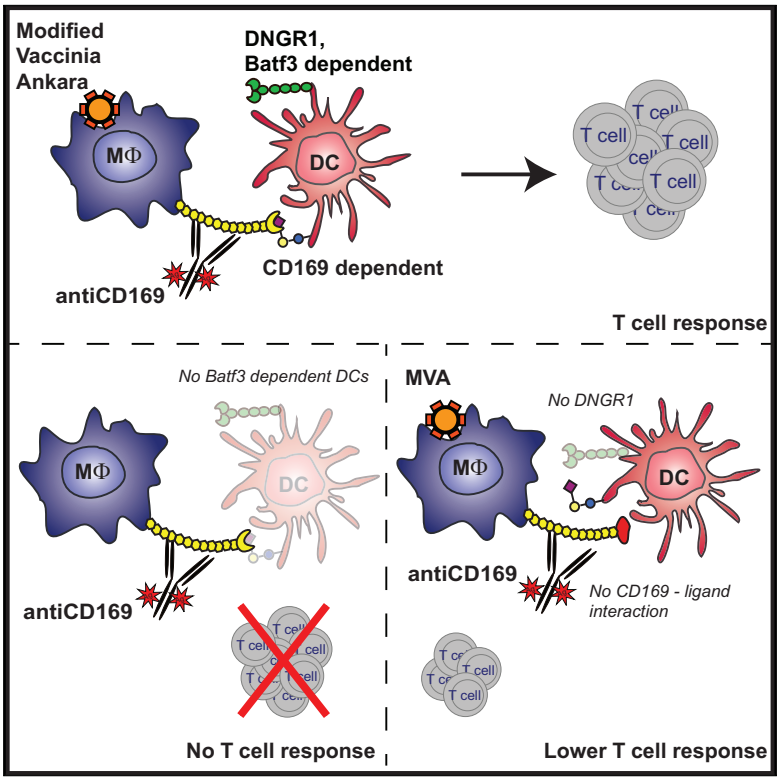

Authors

Dieke van Dinther, Henrike Veninga, Salvador Iborra, ..., David Sancho, Paul R. Crocker, Joke M.M. den Haan

Correspondence

j.denhaan@vumc.nl

In Brief

van Dinther et al. find that splenic CD169$^+$ macrophages transfer antigens to BATF3-dependent cDC1s in a CD169-dependent manner and that these cDC1s cross-prime CD8$^+$ T cell responses in a DNGR-1-dependent manner.

Highlights

- CD169$^+$ macrophages rely on BATF3-dependent DCs to cross-prime CD8$^+$ T cells
- DNGR-1 on cDC1s improves cross-priming to antigens targeted to CD169$^+$ macrophages
- CD169 binds to sialic acids on CD8α^+ DCs
- CD169 binding promotes T cell priming after non-replicative vaccinia virus infection

van Dinther et al., 2018, Cell Reports *22*, 1484–1495
February 6, 2018
https://doi.org/10.1016/j.celrep.2018.01.021

CellPress

OPEN ACCESS
CellPress

Cell Reports
Article

Functional CD169 on Macrophages Mediates Interaction with Dendritic Cells for CD8$^+$ T Cell Cross-Priming

Dieke van Dinther,[1,6] Henrike Veninga,[1,6] Salvador Iborra,[2] Ellen G.F. Borg,[1] Leoni Hoogterp,[1] Katarzyna Olesek,[1] Marieke R. Beijer,[1] Sjoerd T.T. Schetters,[1] Hakan Kalay,[1] Juan J. Garcia-Vallejo,[1] Kees L. Franken,[3] Lamin B. Cham,[4] Karl S. Lang,[4] Yvette van Kooyk,[1] David Sancho,[2] Paul R. Crocker,[5] and Joke M.M. den Haan[1,7,*]

[1]Cancer Center Amsterdam, Department of Molecular Cell Biology and Immunology, VU University Medical Center, Amsterdam, the Netherlands
[2]Immunobiology Laboratory, Centro Nacional de Investigaciones Cardiovasculares Carlos III (CNIC), Madrid, Spain
[3]Department of Immunohematology and Bloodtransfusion, LUMC, Leiden, the Netherlands
[4]Institute of Immunology, Medical Faculty, University Duisburg-Essen, 45122 Essen, Germany
[5]Division of Cell Signalling and Immunology, University of Dundee, Dundee, UK
[6]These authors contributed equally
[7]Lead Contact
*Correspondence: j.denhaan@vumc.nl
https://doi.org/10.1016/j.celrep.2018.01.021

SUMMARY

Splenic CD169$^+$ macrophages are located in the marginal zone to efficiently capture blood-borne pathogens. Here, we investigate the requirements for the induction of CD8$^+$ T cell responses by antigens (Ags) bound by CD169$^+$ macrophages. Upon Ag targeting to CD169$^+$ macrophages, we show that BATF3-dependent CD8α^+ dendritic cells (DCs) are crucial for DNGR-1-mediated cross-priming of CD8$^+$ T cell responses. In addition, we demonstrate that CD169, a sialic acid binding lectin involved in cell-cell contact, preferentially binds to CD8α^+ DCs and that Ag transfer to CD8α^+ DCs and subsequent T cell activation is dependent on the sialic acid-binding capacity of CD169. Finally, functional CD169 mediates optimal CD8$^+$ T cell responses to modified vaccinia Ankara virus infection. Together, these data indicate that the collaboration of CD169$^+$ macrophages and CD8α^+ DCs for the initiation of effective CD8$^+$ T cell responses is facilitated by binding of CD169 to sialic acid containing ligands on CD8α^+ DCs.

INTRODUCTION

While lymph nodes receive antigen (Ag) via the afferent lymph vessels, the spleen filters the blood in the marginal zone and red pulp. Macrophages characterized by high expression of CD169, also known as Sialoadhesin or sialic acid-binding immunoglobulin-like lectin-1 (Siglec-1), are situated at both sites of Ag entry, the subcapsular sinus and marginal sinus (Martinez-Pomares and Gordon, 2012). An intact layer of CD169$^+$ macrophages is necessary for removal of pathogens and prevention of further spreading of infection (Gupta et al., 2016; Iannacone et al., 2010; Junt et al., 2007; Seiler et al., 1997) and they rapidly stimulate several innate lymphoid cell types, thereby promoting an early wave of innate host defense (Barral et al., 2010; Kastenmüller et al., 2012; Kawasaki et al., 2013).

CD169$^+$ macrophages are situated on top of B cell follicles, take up Ag such as immune complexes and viruses, present these Ags in intact form to follicular B cells, and induce germinal center B cell responses (Berney et al., 1999; Carrasco and Batista, 2007; Junt et al., 2007; Phan et al., 2007, 2009; Veninga et al., 2015). However, the role of CD169$^+$ macrophages in the priming of CD8$^+$ T cell responses is debated (Asano et al., 2011; Backer et al., 2010; Bernhard et al., 2015).

CD169$^+$ macrophages are frequently the primary cell type infected during a viral infection (Eloranta and Alm, 1999; Iannacone et al., 2010) and while the CD169 molecule itself acts as a viral receptor (Delputte et al., 2007; Erikson et al., 2015; Puryear et al., 2013; Sewald et al., 2015), CD169$^+$ macrophages are generally considered dispensable for the initiation of T cell responses (Aichele et al., 2003; Winkelmann et al., 2014). CD169$^+$ macrophages have been shown to allow viral replication, which results in high amounts of viral Ags and amplification of T and B cell responses (Honke et al., 2011). This suggests that pathogen uptake and Ag generation are the main functions of CD169$^+$ macrophages, while dendritic cells (DCs) are essential for CD8$^+$ T cell priming (den Haan et al., 2000; Jung et al., 2002; Segura and Amigorena, 2015). In our previous studies, we observed Ag presentation to CD8$^+$ T cells by cross-presenting CD8α^+ DCs (classical DC1, cDC1) when Ag was targeted to CD169$^+$ macrophages (Backer et al., 2010). Recently, Bernhard et al. (2015) showed that after adenoviral infection of CD169$^+$ macrophages, long-lived Ag was cross-presented by CD8α^+ DCs to CD8$^+$ T cells. Together, these studies indicate a functional collaboration between CD169$^+$ macrophages and cross-presenting DCs in the activation of CD8$^+$ T cells and imply an interaction between the two cell types to enable Ag transfer. However, the molecular interactions involved in this process are completely unknown.

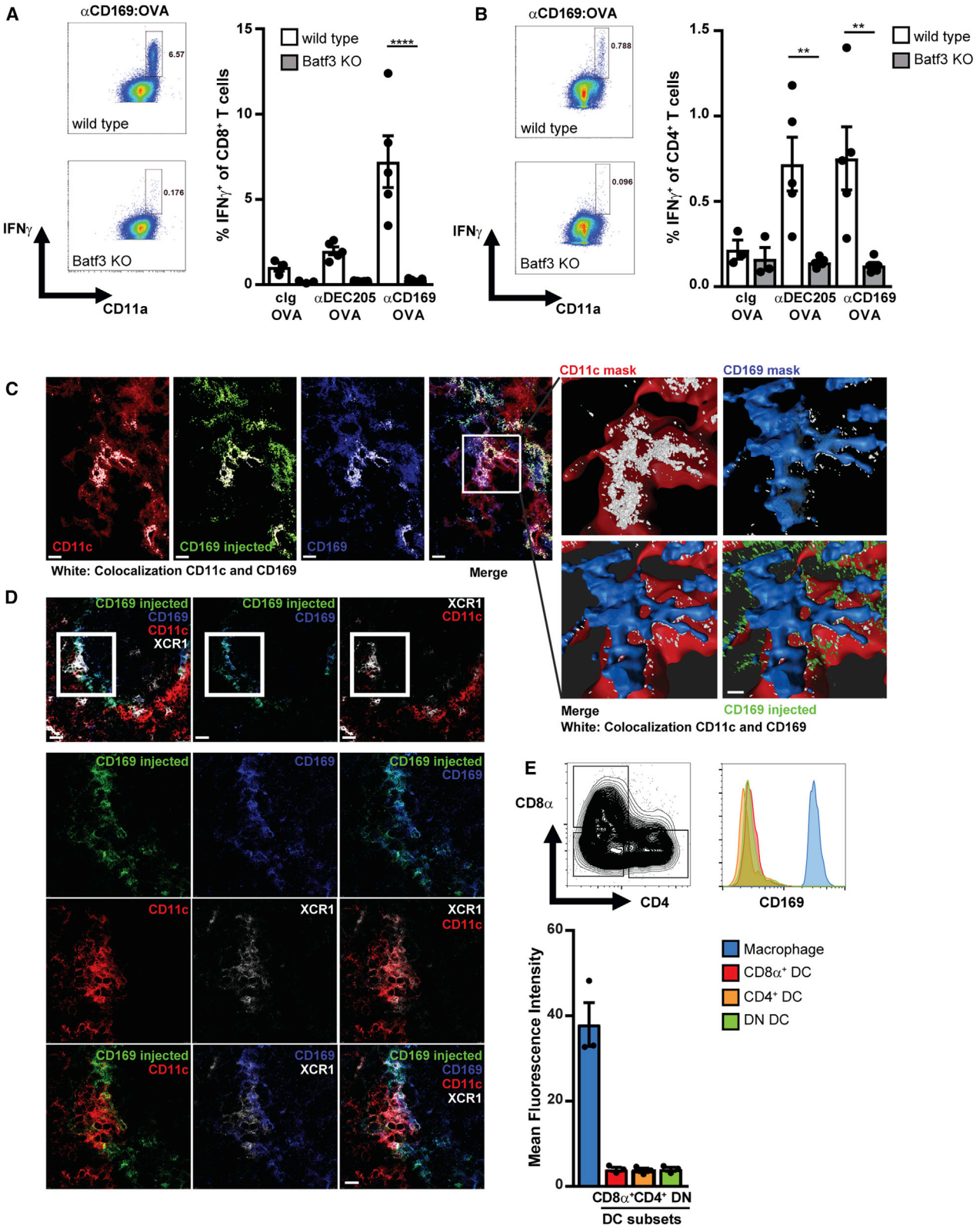

(legend on next page)

One of the molecules indicated to play a role in cellular communication is CD169 itself. CD169 is a lectin receptor that binds sialylated glycoproteins and glycolipids on both endogenous cells as well as pathogens (Crocker and Gordon, 1989; Crocker et al., 1994; Macauley et al., 2014). In previous studies, CD169 has been shown to mediate binding to neutrophils and to innate-like lymphocytes (Crocker et al., 1995; van den Berg et al., 1992; Zhang et al., 2016). In the present study, we find that, when Ags are specifically targeted to CD169$^+$ macrophages, presentation by BATF3-dependent cross-presenting DCs is essential for cross-priming of CD8$^+$ T cells. Our studies demonstrate that CD169 is involved in Ag transfer to CD8α^+ DCs and priming of CD8$^+$ T cells. Finally, the activation of non-replicative vaccinia virus-specific CD8$^+$ T cells is hampered when the binding activity of CD169 was blocked. These results indicate that CD169$^+$ macrophages interact with DC1s in a CD169-dependent manner and that this interaction enhances BATF3-dependent, DNGR-1-mediated cross-priming of CD8$^+$ T cells.

RESULTS

T Cell Responses after Ag Targeting to CD169$^+$ Macrophages Rely on BATF3-Dependent DCs

Previously, we showed that Ag targeting to CD169$^+$ macrophages resulted in Ag presentation by CD8α^+ DCs to CD8$^+$ T cells (Backer et al., 2010). To investigate the requirement of cross-presenting DCs to present Ags bound by CD169$^+$ macrophages, we used BATF3-deficient mice, which contain significantly decreased numbers of cross-presenting CD8α^+ DCs, but do contain normal frequencies of CD169$^+$ macrophages (Figures S1A and S1B) (Hildner et al., 2008). We immunized wild-type (WT) and BATF3-deficient mice with antibody (Ab)-ovalbumin (OVA) conjugates targeted to DEC205$^+$CD8α^+ DCs or CD169$^+$ macrophages in the presence of adjuvants. Both OVA targeting to DEC205 or CD169 induced OVA-specific effector and memory CD8$^+$ and CD4$^+$ T cells in a BATF3-dependent manner (Figures 1A, 1B, and S1C). These results demonstrate that CD169$^+$ macrophages do not cross-present exogenous Ags and that T cell cross-priming relies on cross-presenting DCs.

Because Ag transfer between CD169$^+$ macrophages and DCs would imply physical interactions between these cells, we determined the localization of DCs and CD169$^+$ macrophages in mice injected with Alexa 488-labeled anti-CD169 (αCD169-488) Ab plus adjuvant by fluorescence microscopy. DCs and CD169$^+$ macrophages were located in close contact with each other, and the injected Ab was observed on contact points between the macrophages and the DCs (Figure 1C). Staining for XCR1, which is a unique marker for BATF3-dependent DCs, demonstrated multiple interactions between XCR1$^+$ cDC1s with CD169$^+$ macrophages carrying CD169-488 (Figure 1D). Together, these results indicate colocalization between CD169$^+$ macrophages and cross-presenting DCs, and we hypothesize that this interaction would enable Ag transfer.

We and others have observed that CD8α^+ DCs show some CD169 staining after isolation using enzymatic digestion (Figure S1D) (Segura et al., 2010). If CD8α^+ DCs would express CD169 molecules, then direct targeting to DCs would be possible. However, we and others did not detect CD169 RNA expression in sorted CD8α^+ DCs (Figure S1E) (GEO: GSE6259) (Dudziak et al., 2007). The presence of CD169 on other cell types can be caused by the isolation procedure (Zhang et al., 2016). To exclude this phenomenon, we used multiplex confocal microscopy, 3D image surface rendering, and subsequent histocytometry analysis of murine spleens to quantify CD169 expression *ex vivo* on APC subsets. This analysis showed no expression of CD169 by DC subsets in spleen sections (Figure 1E). Together, these results suggest that CD8α^+ DCs do not express CD169, but do interact with CD169$^+$ macrophages and are essential for the activation of CD8$^+$ T cell responses.

Ags Bound by CD169$^+$ Macrophages Are Transferred to CD8α^+ DCs

To investigate Ag transfer between CD169$^+$ macrophages and DCs, we analyzed the transfer of αCD169-488 to DCs in the presence of adjuvant by flow cytometry. At 10 min after injection, half of the macrophages were labeled with fluorescent Ab (Figures S2A and S2B), while this was negligible for CD8α^+, CD4$^+$, or double negative (DN) DCs (Figures 2A–2C). Two hours after immunization, 75% of the macrophages (Figures S2A and S2B) and 15%–20% of CD8α^+ DCs and DN DCs, and to a lower extent CD4$^+$ DCs, were labeled (Figures 2A–2C). The increase in mean fluorescence was highest in CD8$^+$ DCs at different time points after injection (Figure 2D). Analysis of transferred αCD169-488 in DC subsets in BATF3-deficient mice revealed an increase in Ag transfer to CD4$^+$ DCs (Figures 2E–2H). These results suggest a preferential interaction between CD169$^+$ macrophages with CD8α^+ DCs.

Figure 1. T Cell Activation after Ag Targeting to CD169$^+$ Macrophages Requires BATF3-Dependent DCs

(A and B) Percentage of OVA-specific IFNγ producing CD8$^+$ (A) and CD4$^+$ (B) CD11a$^+$ T cells after *in vitro* re-stimulation with H-2K^b-restricted OVA$_{257–264}$ peptide or I-A^b-restricted OVA$_{262–276}$ peptide, in C57BL/6 (WT, wild-type) and BATF3-deficient knockout (KO) mice 9 days after immunization (1 μg of indicated Ab-OVA with 25 μg αCD40 and 25 μg poly(I:C)). Representative flow cytometry plots and mean ± SEM of one representative experiment of two experiments using 3–5 mice/group. Statistical analysis one-way ANOVA with Bonferroni's multiple comparison test. *p < 0.05, **p < 0.01, ***p < 0.001, ****p < 0.0001; n.s., non-significant.

(C) CD11c (red), injected anti-CD169 (green), CD169 (blue), and in white a co-localization mask of CD11c and CD169 (merge without co-localization mask). Zoom of the indicated area with cell masks for CD11c (red) and CD169 (blue), co-localization mask (white), and injected anti-CD169 (green). Scale bars, 5 μm and 3 μm in the zoom.

(D) Representative image of CD169$^+$ macrophage interacting with XCR1$^+$ DC. CD11c (red), injected anti-CD169 (green), CD169 (blue), and XCR1 (white). Scale bars, 25 μm and 10 μm in the zoom.

(E) *In situ* CD169 expression on splenic macrophages and DC subsets based on multiplex confocal microscopy and 3D image surface rendering of whole spleen sections (n = 3).

See also Figure S1F.

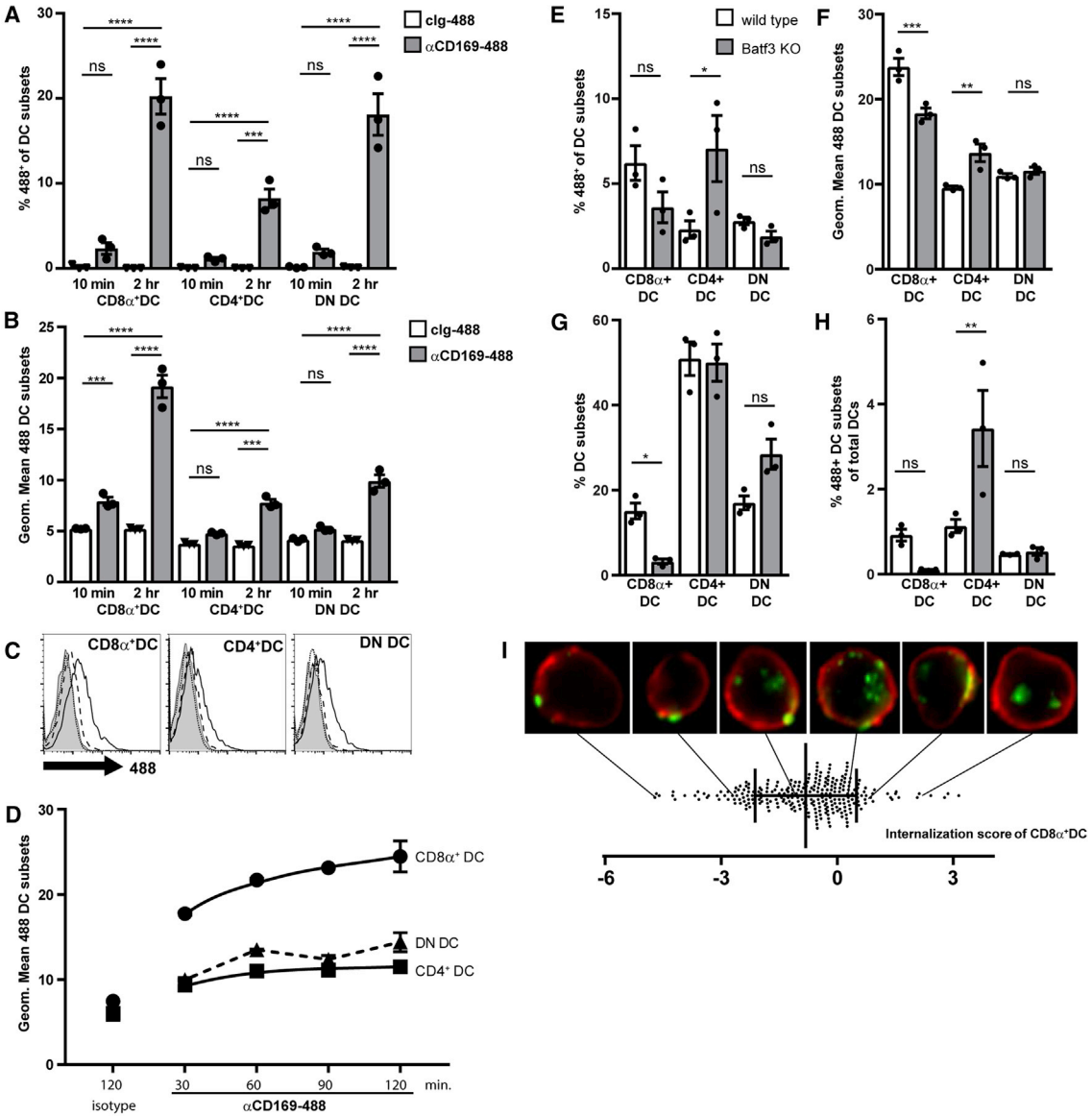

Figure 2. Ags Targeted to CD169$^+$ Macrophages Are Transferred to DCs

(A–D) Wild-type mice were injected with 1 μg of the indicated Ab-Alexa488 with 25 μg αCD40 and 25 μg poly(I:C). (A) Percentage of Alexa488$^+$ DCs, (B) geometric mean of Alexa488 signal per DC subset, and (C) representative histogram of each DC subset at 10 min (dotted line) and 2 hr (solid line) after immunization (gray line isotype control), one representative experiment of two experiments each with 3 mice/group. (D) Geometric mean ± SEM of Alexa488 signal per DC subset on indicated time points after injection. 3 mice/group.

(E–H) Wild-type mice or BATF3-KO mice were injected with 1 μg of the indicated Ab-Alexa488 with 25 μg αCD40 and 25 μg poly(I:C). (E) Percentage of Alexa488$^+$ DCs and (F) geometric mean of Alexa488 signal per DC subset. (G) percentage of DC subsets per group. (H) 488$^+$ cells per subset as a percentage of total DCs. Mean ± SEM of one representative experiment of two with 3 mice per group.

(I) Representative images of isolated CD8α$^+$ DCs containing Alexa488 signal 2 hr after Ag targeting. 3 mice per group were pooled, representative of 4 experiments. Negative internalization scores indicate that the majority of Alexa488 signal is membrane-associated, while positive internalization scores indicate intracellular presence of Alexa488 signal. Statistical analysis one-way ANOVA with Bonferroni's multiple comparison test. *$p < 0.05$, **$p < 0.01$, ***$p < 0.001$, ****$p < 0.0001$; n.s., non-significant.

Using imaging flow cytometry, CD8α$^+$ DCs were shown to carry both membrane-associated and intracellular fluorescent content, indicating uptake of αCD169-488 (Figure 2I). The fluorescence was concentrated in round structures both at the cell membrane as well as intracellular, which is in line with the observed binding and uptake of cellular vesicles during the 2 hr after immunization. The combined results of these studies indicate that Ags are transferred from CD169$^+$ macrophages to DCs, and the transfer appears to be more efficient to CD8α$^+$ and to DN DCs than to CD4$^+$ DCs.

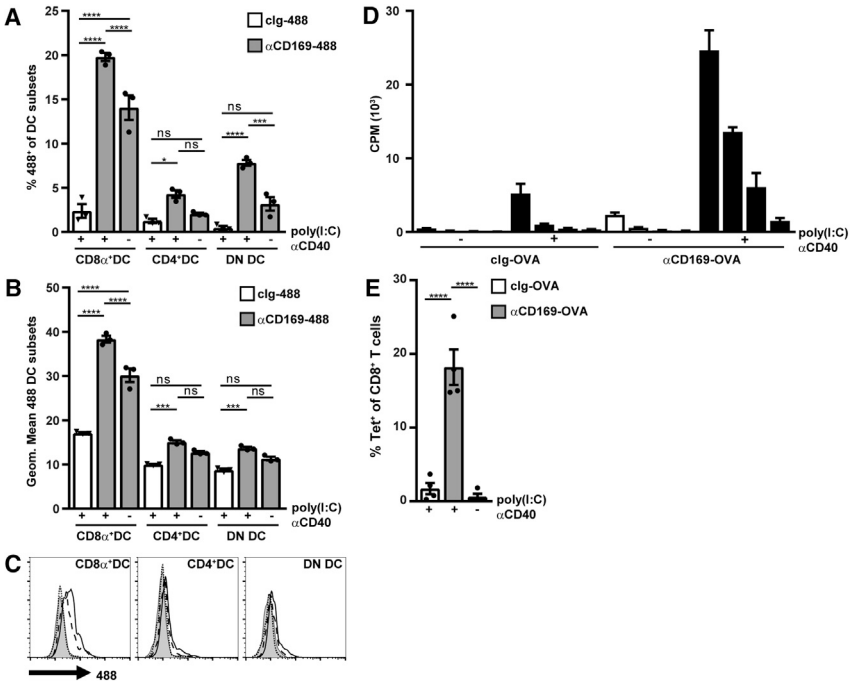

Figure 3. Adjuvant Enhances Antigen Transfer from Macrophages to DCs

(A–C) Wild-type mice were injected with 1 μg of the indicated Ab-Alexa488 in the presence or absence of 25 μg αCD40 and 25 μg poly(I:C). (A) Percentage of Alexa488$^+$ DC subsets and (B) geometric mean of Alexa488 signal per DC subset 2 hr after injection using 3 mice/group. (C) Representative histograms of each DC subset at 2 hr after injection of Ab-Alexa488 with adjuvant (solid line) or without adjuvant (dotted line), gray area for the isotype control. Mean ± SEM of one representative of 2 experiments is shown.

(D) Wild-type mice were injected with 1 μg of indicated Ab-OVA in the presence or absence of 25 μg αCD40 and 25 μg poly(I:C). 16 hr later DCs were used as stimulators for an OT-I proliferation assay, measured by ^{3}H-Thymidine incorporation. Graph shows mean counts per minute (CPM) ± SEM of triplicate co-cultures of 10^5 OT-I T cells together with a 3-fold 3-step titration of DCs starting at 2.5 × 10^5 DCs. One representative experiment of 3 is shown.

(E) Percentage of H-2K^b-SIINFEKL-tetramer$^+$ CD8$^+$ T cells 7 days after immunization. Mean ± SEM of 3 mice per group. Statistical analysis one-way ANOVA with Bonferroni's multiple comparison test. *p < 0.05, **p < 0.01, ***p < 0.001, ****p < 0.0001; n.s., non-significant.

Adjuvant Enhances Ag Transfer from CD169$^+$ Macrophages to CD8α$^+$ DCs

Because all previous experiments were performed in the presence of adjuvant, we questioned whether Ag transfer was enhanced by the presence of adjuvant. We detected a decrease in the percentage and intensity of fluorescent CD8α$^+$ and DN DCs in mice injected with αCD169-488 without adjuvant, although still a significant amount of Ag transfer remained (Figures 3A–3C). To test the functional relevance of Ag transfer in the absence of adjuvant, we used DCs from mice injected with αCD169-OVA without adjuvant to stimulate OT-I T cells *in vitro*. These DCs provided minimal stimulation for OT-I T cell activation, even though they could stimulate T cell responses after exogenous peptide loading, indicating that the DCs did not have any intrinsic defect to stimulate T cells (Figures 3D and S3A). In addition, immunization with αCD169-OVA conjugate in the absence of adjuvant did not lead to OVA-specific T cell responses *in vivo* (Figure 3E). Our results demonstrate that adjuvant enhances Ag transfer from CD169$^+$ macrophages to DCs and is absolutely essential in the activation of T cell responses.

DNGR-1 Expression on Cross-Presenting DCs Enhances Cross-Priming of CD8$^+$ T Cell Responses

A well-known feature of CD8α$^+$ DCs is that they can efficiently recognize and cross-present cell-associated Ags from dying cells (den Haan et al., 2000; Iyoda et al., 2002; Schulz and Reis e Sousa, 2002). Recently, lymph node CD169$^+$ macrophages were shown to die and disappear after infection or inflammation (Gaya et al., 2015; Sagoo et al., 2016). Consistent with this, we detected a significant decrease in CD169$^+$ macrophages and migration of the remaining CD169$^+$ macrophages into the B cell follicles 24 and 48 hr after adjuvant injection, while αCD169-OVA conjugate in the absence of adjuvant did not induce this disappearance (Figure 4A). Because macrophages also quickly die following isolation (Zhang et al., 2016) (Figure S4A), we hypothesized that they might die upon activation *in vivo* and that this process would enhance recognition by CD8α$^+$ DNGR-1-expressing DCs. DNGR-1 is a C-type lectin receptor that recognizes F-actin on dead cells and stimulates cross-presentation of dead-cell-derived material by CD8α$^+$ DCs and the activation of CD8$^+$ T cell responses in viral infections (Ahrens et al., 2012; Iborra et al., 2012, 2016; Sancho et al., 2009). Normal numbers of both CD169$^+$ macrophages and DC were detected in DNGR-1-deficient (Clec9agfp/gfp) mice (Figure S4B). While Ag transfer from CD169$^+$ macrophages to DCs was unaffected in DNGR-1-deficient mice (Figures 4B and 4C), CD8$^+$ T cell responses were significantly lower in DNGR-1-deficient mice following immunization (Figures 4D and 4E). These results are in line with previous studies that demonstrated that DNGR-1 recognition of F-actin is not essential for uptake, but enhances cross-presentation of cell-associated Ag to T cells (Sancho et al., 2009; Zelenay et al., 2012). In conclusion, our data indicate that adjuvants play a relatively minor role in Ag transfer, but are essential for the activation of CD8$^+$ T cell responses and may stimulate DNGR-1-mediated cross-priming of T cells by CD8α$^+$ DC.

CD169 Binds to Sialic Acids on CD8α$^+$ DCs, Promotes Ag Transfer, and T Cell Cross-Priming

The CD169 molecule is a sialic acid binding lectin with a preference for α2,3-linked sialic acids that is involved in cellular interactions (Crocker et al., 1995; van den Berg et al., 1992). We hypothesized a role for CD169 in DC interaction and Ag transfer and stained splenocytes with plant lectins that have a

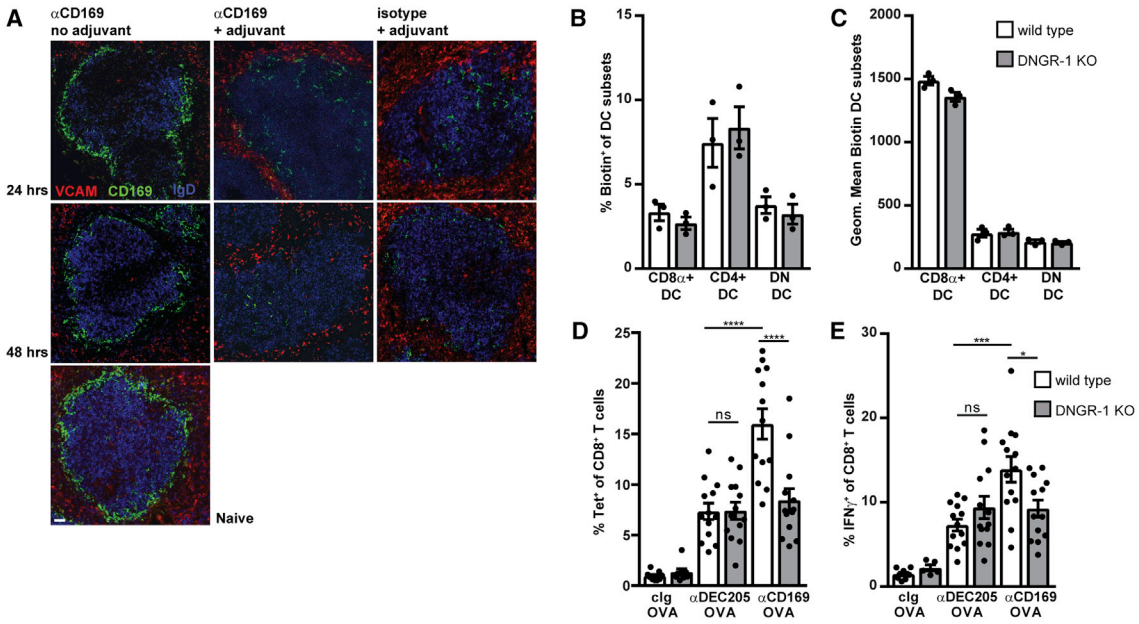

Figure 4. DNGR-1 Expression on Cross-Presenting DCs Enhances Cross-Priming of CD8$^+$ T Cell Responses

(A) Immunofluorescence staining of spleen sections for CD169$^+$ macrophages on different time points after immunization (blue IgD, green CD169, red VCAM; three mice per group). Left: without adjuvant. Middle: with adjuvant and anti-CD169. Right: with adjuvant and isotype control Ab. One representative picture of 3 mice/group is shown. Scale bar, 30 μm.

(B and C) Wild-type mice or DNGR1$^{gfp/gfp}$ mice were injected with 1 μg of the indicated Ab-biotin with 25 μg αCD40 and 25 μg poly(I:C). (B) Percentage of biotin$^+$ DCs and (C) geometric mean of biotin signal per DC subset. Mean ± SEM of one representative experiment of two with three mice per group is shown.

(D and E) Percentage of H-2K^b-SIINFEKL-tetramer$^+$ CD8$^+$ T cells (D) and percentage of OVA-specific IFNγ-producing CD8$^+$ T cells (E) after *in vitro* re-stimulation with H-2K^b-restricted OVA$_{257–264}$ peptide in C57BL/6- or DNGR-1-deficient mice 7 days after immunization. Graphs show mean ± SEM of 2 experiments combined using 15 mice/group. Statistical analysis one-way ANOVA with Bonferroni's multiple comparison test. *p < 0.05, **p < 0.01, ***p < 0.001, ****p < 0.0001; n.s., non-significant.

specificity for α2,3 sialic acids (MAL-II) and α2,6 sialic acids (SNA) (Figure 5A). DCs showed highest expression of α2,3 sialic acids compared to B cells and neutrophils, and low expression of α2,6 sialic acids. Recombinant CD169Fc proteins demonstrated more binding to DCs than to neutrophils (Figure 5B). Especially CD8α$^+$ and to a lesser extent CD4$^+$ and DN DCs bound MAL-II (Figure 5C) and recombinant CD169Fc (Figure 5D). Binding was dependent on sialic acids as neuraminidase treatment of DCs abrogated the interaction (Figure 5E) and recombinant CD169Fc containing an alanine substitution in the sialic acid binding domain (R97A) that abolishes sialic acid binding, did not bind to DCs or to other splenocytes (Figures 5B and 5D) (Vinson et al., 1996). These data indicate that CD169 on macrophages can bind to sialic acids on DCs and this may facilitate the interaction between macrophages and DCs necessary for the transfer of CD169$^+$ macrophage-derived Ag to cross-presenting CD8α$^+$ DCs.

To investigate the role of CD169-mediated recognition of sialic acids in the transfer of Ag and the activation of T cells, we injected Sn-KI mice expressing a mutated CD169, unable to bind sialic acids because of the amino acid substitutions R97A and W2Q, with αCD169-488 and measured the transfer of αCD169-488 to DCs 2 hr after injection (Klaas et al., 2012). Sn-KI mice contain normal numbers of the DC subsets and CD169-expressing macrophages (Figures S5A–S5C). Both the percentage of Alexa488$^+$ DCs and the MFI on the DC subsets were decreased by 50% or more in Sn-KI mice (Figures 6A and 6B). This indicates that Ag transfer between CD169$^+$ macrophages and DCs depends on the presence of functional sialic-acid binding CD169 on the macrophages. Accordingly, CD8$^+$ and CD4$^+$ T cell responses following immunization with αCD169-OVA conjugates were reduced in Sn-KI mice compared to wild-type mice, whereas immunization with αDEC205-OVA conjugates was not affected (Figures 6C and 6D). These experiments show that CD169 binds to CD8α$^+$ DCs in a sialic acid-dependent manner, and functional CD169 enhances Ag transfer and contributes to T cell cross-priming *in vivo*.

Uptake of Soluble Ag and Immune Complexes by DCs Is Not Dependent on Functional CD169

To determine whether functional CD169 is important for other types of Ag, we investigated the uptake of soluble antigen and immune complexes by DC subsets in wild-type and Sn-KI mice. Two hours after injection of Alexa 488-labeled OVA, a similar percentage of all DC subsets was Alexa488-positive and this was not changed in Sn-KI mice (Figures 6E, 6F, and S6A). Similarly, the uptake of immune complexes of OVA-488 rabbit anti-OVA Ab was present in all DC subsets and not affected by a non-functional CD169 molecule (Figures 6G, 6H,

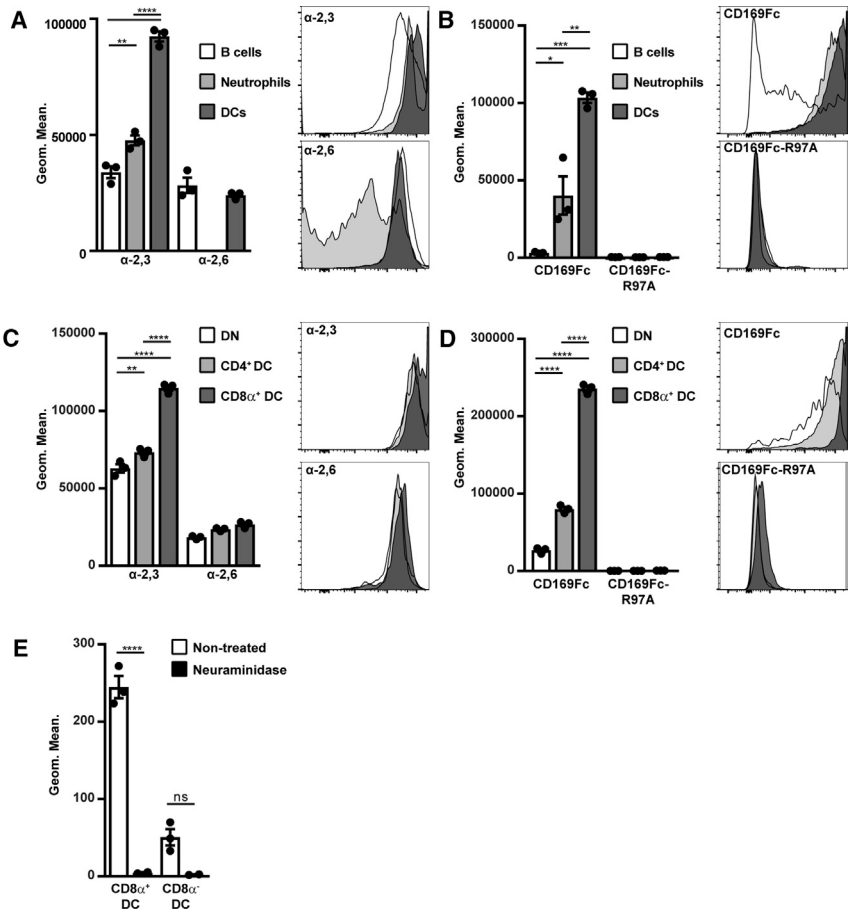

Figure 5. CD169 Binds to CD8α$^+$ DCs in a Sialic Acid-Dependent Manner

(A–D) Binding of MAL-II and SNA lectins (α2,3 and α2,6-sialic acid specific) and recombinant CD169-1Fc and CD169-R97A mutant to B220$^+$ B cells, Gr1$^+$ CD11b$^+$ neutrophils, and CD11c$^+$MHC class II$^+$ DCs (A) and (B) and to CD8$^+$ and CD8$^-$ CD11c$^+$ MHC class II$^+$ DCs (C) and (D).

(E) Binding of CD169-Fc to neuraminidase-treated and non-treated DCs.

Geometric mean ± SEM of 3 mice/group and one representative experiment from at least two independent experiments is shown. Statistical analysis one-way ANOVA with Bonferroni's multiple comparison test. *p < 0.05, **p < 0.01, ***p < 0.001, ****p < 0.0001; n.s., non-significant.

and S6B). These results suggest that DCs directly take up soluble Ag and immune complexes independently of CD169-mediated interaction with macrophages.

Blocking CD169 Interactions Impairs T Cell Responses after Modified Vaccinia Ankara Virus Infection

CD8$^+$ T cell responses induced by modified vaccinia Ankara (MVA) virus infection are dependent on BATF3-dependent cross-presenting DCs and DNGR-1-mediated cross-priming (Iborra et al., 2012, 2016). MVA infects CD169$^+$ macrophages in lymph nodes and induces cell death (Sagoo et al., 2016). We infected mice with MVA virus in the footpad and analyzed the effect of CD169-blocking antibodies on the MVA-specific CD8$^+$ T cell response in the draining lymph node and spleen 7 days after infection. The CD169-blocking Abs did not affect CD169$^+$ macrophage presence in spleen and lymph node (Figure S6B). We observed significantly decreased T cell responses specific for the B8R immunodominant peptide from MVA in both lymph nodes as well as spleen as detected by tetramer staining and intracellular cytokine staining after *in vitro* restimulation, which indicates that functional CD169 is necessary to mediate cross-priming of MVA-specific CD8$^+$ T cells (Figures 7A–7C). Moreover, we found a significant decrease in KLRG-1^{low} cells when CD169 was blocked (Figure 7D), fitting with a decrease in Ag cross-presentation and limited CD4$^+$ T cell help via BATF3-dependent DCs (Eickhoff et al., 2015), while the numbers of KLRG-1^{high} cells were not affected (Figure 7E). Together, our results indicate that in MVA vaccinia virus infection functional CD169 is necessary to obtain optimal cross-presentation and induction of CD8$^+$ T cell responses.

In contrast to T cell responses after MVA infection, T cell responses after intravenous vesicular stomatitis virus infection were not influenced by blocking CD169-binding to its ligands (Figure S6C). In conclusion, our analysis of two different viral models suggest that CD169-mediated interaction between CD169$^+$ macrophages and CD8α$^+$ DCs contributes to the generation of CD8$^+$ T cell immunity in those viral infections in which cross-presentation is essential.

DISCUSSION

CD169$^+$ macrophages in lymphoid organs are the first cells to bind incoming pathogens and act as gatekeepers to prevent further dissemination of pathogens. While their excellent capacity to present Ags to B cells is well established, their specific role in the activation of T cell responses and the molecular mechanisms of their interaction with cross-presenting DCs are still not known. Our studies demonstrate unequivocally that BATF3-dependent DCs and CD169$^+$ macrophages have a CD169-dependent interaction that facilitates Ag transfer and DNGR1-mediated cross-presentation and thereby enables the efficient induction of CD8$^+$ T cell responses to viruses that depend on cross-presentation.

Interestingly, a recent study on human DCs describes a division of labor between DC subsets in which Ag acquisition and Ag presentation functions are separated over different DC subsets (Silvin et al., 2017). We propose a similar division of labor for CD169$^+$ macrophages and BATF3-dependent cross-presenting DCs in the mouse. Multiple studies have illustrated that CD169$^+$ macrophages bind and are infected by different

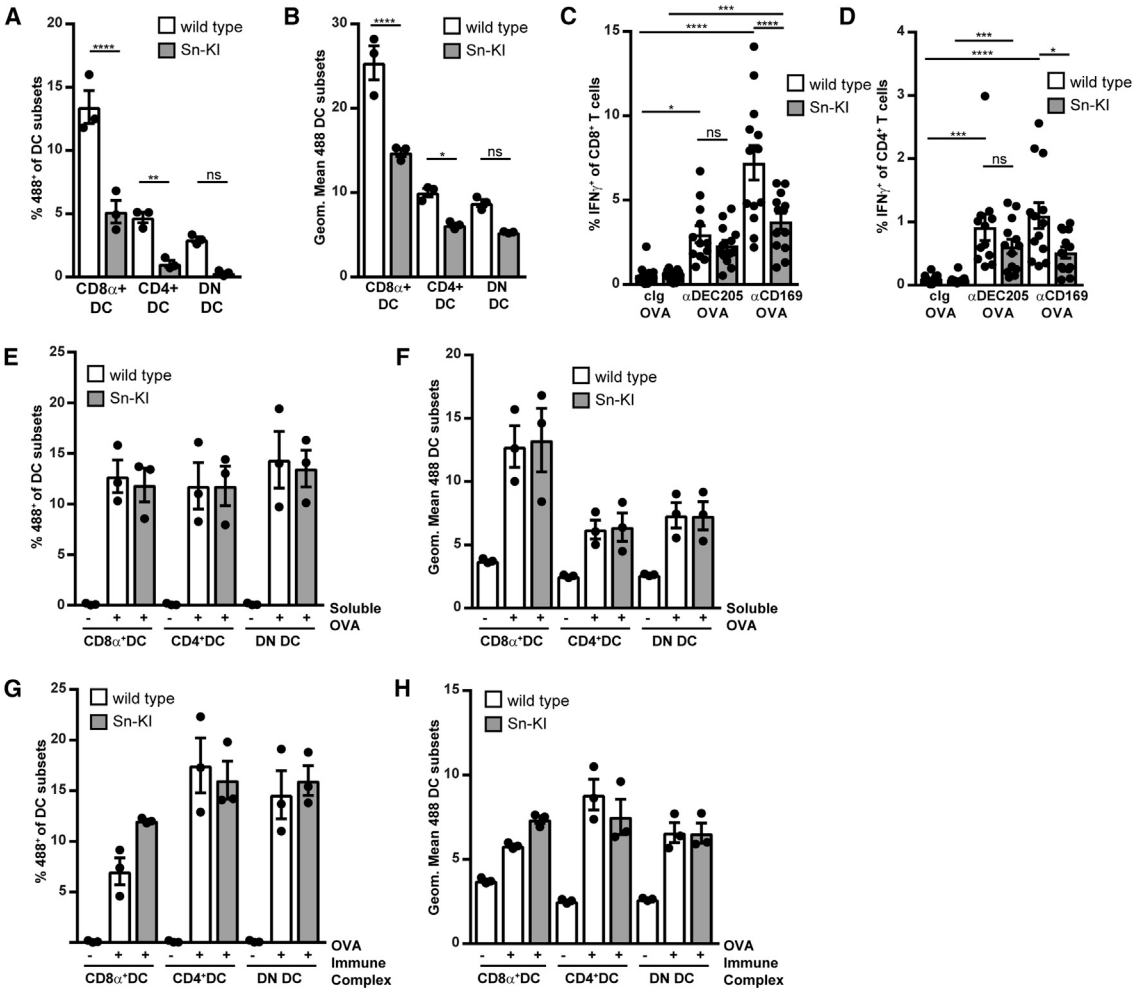

Figure 6. CD169 Promotes Ag Transfer and T Cell Cross-Priming

(A and B) Wild-type or Sn-KI mice were injected with 1 μg of the indicated Ab-488 with 25 μg αCD40 and 25 μg poly(I:C). (A) Percentage of Alexa488$^+$ DC subsets and (B) geometric mean of Alexa488 signal per DC subset two hours after injection using 3 mice/group. Mean ± SEM of one representative of 2 experiments is shown.

(C and D) Percentage of OVA-specific IFNγ-producing CD8$^+$ (C) and CD4$^+$ (D) CD11a$^+$ T cells after *in vitro* re-stimulation with H-2K^b-restricted OVA$_{257–264}$ peptide or I-A^b-restricted OVA$_{262–276}$ peptide, respectively, in spleens of wild-type and Sn-KI mice 9 days after immunization with 1 μg of indicated Ab-OVA with 25 μg αCD40 and 25 μg poly(I:C). Graphs show the combined mean ± SEM from 3 experiments of total 13 mice/group.

(E and F) Wild-type or Sn-KI mice were injected with 100 μg rabbit-anti-OVA Ab and 30 min later with 5 μg soluble Alexa488-labeled OVA, resulting in the formation of immune complexes.

(G and H) Wild-type or Sn-KI mice were injected with 50 μg soluble Alexa488-labeled OVA.

(E–H) Percentage of Alexa488$^+$ DC subsets (E and G) and geometric mean of Alexa488 signal per DC subset (F and H) 2 hr after injection using 3 mice/group. Mean ± SEM of one representative of two experiments is shown. Statistical analysis one-way ANOVA with Bonferroni's multiple comparison test. *p < 0.05, **p < 0.01, ***p < 0.001, ****p < 0.0001; n.s., non-significant.

types of viruses (Bernhard et al., 2015; Honke et al., 2011; Junt et al., 2007; Sagoo et al., 2016; Sewald et al., 2015). In the case of VSV infection, this leads to enhanced local restricted replication of the virus and the production of Ag that enhances B and T cell responses (Honke et al., 2011). Vaccinia virus infection of CD169$^+$ cells has been shown to lead to inflammasome activation and cell death (Sagoo et al., 2016). Bacterial infection and inflammatory agents induced disappearance of subcapsular sinus CD169$^+$ macrophages in the lymph node (Gaya et al., 2015). Similarly, we observed the disappearance of splenic marginal zone CD169$^+$ macrophages after injection with adjuvant. Although we formally did not show CD169$^+$ macrophage cell death, we hypothesized that adjuvant-induced macrophage cell death would lead to generation of ligands for DNGR-1 expressed on Batf-3-dependent DCs that would enable cross-presentation of cell-associated antigens (Ahrens et al., 2012; Iborra et al., 2012; Sancho et al., 2009; Zelenay et al., 2012). Indeed, experiments in DNGR-1-deficient mice demonstrated a role for DNGR-1 in the cross-priming of T cell responses after Ag targeting to CD169$^+$ macrophages, although we did not observe a major role for adjuvant or DNGR-1 for Ag transfer to DCs as has been previously reported (Iborra et al., 2012).

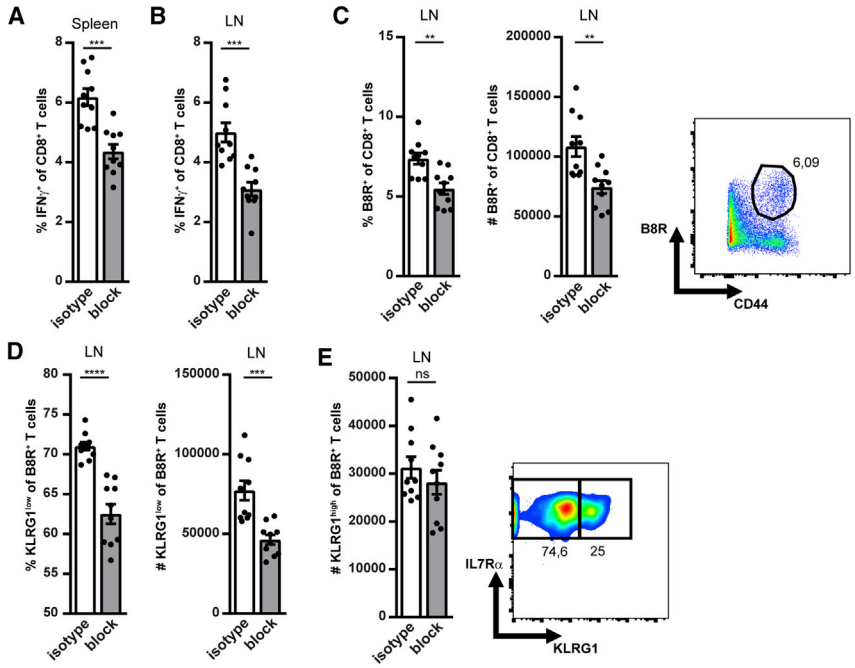

Figure 7. *In Vivo* Blockade of CD169 Impairs the Activation of MVA-Specific CD8$^+$ T Cell Responses

(A–D) Percentage of MVA-specific IFNγ-producing CD8$^+$ T cells in spleen (A) and LNs (B) after *in vitro* re-stimulation with MVA-derived B8R$^+$ peptide 7 days after footpad infection with 5 × 10^5 PFU MVA in the presence of CD169-blocking Abs or isotype control. Percentage and number of B8R$^+$ tetramer-specific CD8$^+$ T cells (C) and of KLRG1^{low} B8R$^+$ CD8$^+$ T cells (D) in LNs from mice 7 days after footpad infection. (E) Number of KLRG1^{high} B8R$^+$ CD8$^+$ T cells in LNs from mice 7 days after footpad infection with 5 × 10^5 PFU MVA. Representative plots and mean ± SEM from the combined data of two independent experiments with a total of 10 mice/group are shown. Statistical analysis Student's t test. *p < 0.05, **p < 0.01, ***p < 0.001, ****p < 0.0001; n.s., non-significant.

Previously, CD169 was implicated in mediating binding of CD169$^+$ macrophages to lymphocytes, neutrophils, and innate lymphocytes (Crocker et al., 1995; van den Berg et al., 1992; Zhang et al., 2016). Here, we show strong CD169 binding to DCs, and we propose that this adhesive function promotes Ag transfer especially to BATF3-dependent CD8α$^+$ cross-presenting DCs. This pathway will possibly be less relevant for those Ags and viruses that are likely to be taken up directly by DCs, such as soluble Ag, immune complexes, and VSV. DCs express multiple Fcγ and complement receptors that enable immune complex uptake and cross-presentation (den Haan and Bevan, 2002; van Montfoort et al., 2007). In addition, effector T cell priming after VSV infection has been previously shown not to require CD169$^+$ macrophages (Ciavarra et al., 1997; Honke et al., 2011; Iannacone et al., 2010). Interestingly, a recent study demonstrated that specifically memory CD8$^+$ T cell responses for VSV were dependent on XCR1$^+$ cross-presenting DCs and their interaction with CD169$^+$ macrophages (Habbeddine et al., 2017). Collectively, these studies indicate that XCR1$^+$ BATF3-dependent CD8α$^+$ cross-presenting DCs are differentially required for effector and memory CD8$^+$ T cell responses in different viral infections. Our results with the non-replicative vaccinia virus infection model suggest that effector and memory T cell responses that are dependent on cross-presenting DCs may be influenced by CD169-mediated transfer of Ag.

Presentation by BATF3-dependent DCs serves as a platform for CD4$^+$ T cell help that is necessary for the generation of long-term CD8$^+$ T cell memory responses and mediates generation of CD8$^+$ T cell resident memory responses (Eickhoff et al., 2015; Hor et al., 2015; Iborra et al., 2016). Ag transfer from CD169$^+$ macrophages to BATF3-dependent DCs would optimally facilitate the generation of these (resident) memory CD8$^+$ T cell responses. Indeed, we observed a decrease in KLRG-1^{low} Ag-specific CD8$^+$ T cells, considered to have received CD4$^+$ T cell help, when CD169 interaction was blocked during vaccinia virus. This would imply that Ag transfer from CD169$^+$ macrophages to BATF3-dependent DCs is not only essential for the generation of effector CD8$^+$ T cell responses, but also enables CD4$^+$ T cell help and long-term memory T cell responses.

In conclusion, we demonstrate that CD169$^+$ macrophages interact with cross-presenting CD8α$^+$ DCs in a CD169-dependent manner and thereby enable Ag transfer, DNGR-1 stimulation, and the cross-priming of CD8 T cell responses. We propose that this collaboration is optimized for Ag acquisition and Ag presentation to T cells, is physiologically relevant, and could also be exploited for vaccination purposes.

EXPERIMENTAL PROCEDURES

Preparation of Monoclonal Antibody-OVA Conjugates

Purified rat IgG2a Ab αCD169 (MOMA-1), αDEC205 (NLDC145), and isotype control (R7D4) were activated with SMCC (Pierce). Lipopolysaccharide (LPS)-free OVA (Seikagaku) was functionalized with SATA (Pierce). After removal of excess reagent and deacetylation of SATA, Abs were conjugated with 5 equivalents (molar ratios) of OVA. Unconjugated OVA was removed by gel filtration using a Superdex 200 column (Amersham).

Mice

C57Bl6/J, BATF3-deficient, and OT-I mice were obtained from Charles River or the Jackson Laboratory. Sn-KI mice in which Trp2 and Arg97 from CD169 were changed to Gln and Ala, respectively, were generated at the University of Dundee, and bred at the animal facility of the VU University Medical Center (Klaas et al., 2012). *Clec9a$^{gfp/gfp}$* mice were bred at the animal facility of the CNIC in Madrid, Spain (Sancho et al., 2009). All mice used in this study were matched for age (8–12 weeks) and sex and kept under specific pathogen-free conditions. Experiments were approved by the Animal Ethics Committees of our institutes.

Immunizations

Mice were immunized intravenously (i.v.) with 1 μg monoclonal antibody (mAb)-OVA in the presence or absence of 25 μg poly(I:C) and 25 μg αCD40 Ab (clone 1C10). Wild-type mice were treated with CD169-blocking Ab (mix of 200 μg SER-4 and 100 μg 3D6) or isotype control Ab (300 μg R7D4) at (day −1 or −2) and infected i.v. with 2 × 10^6 plaque-forming unit (PFU) of

VSV or infected in the footpad with 5 × 10^5 PFU MVA. MVA-GFP was kindly provided by Mariano Esteban (Di Pilato et al., 2013). VSV (Indiana strain, Mudd-Summers isolate) was originally obtained from D. Kolakofsky. Virus was propagated on BHK-21 hamster kidney fibroblasts at a MOI of 0.01.

Flow Cytometry

Stainings were performed after blocking Fc receptors with clone 2.4G2 for 30 min at 4°C. For intracellular staining, cells were fixed in PBS containing 2% paraformaldehyde and stained in PBS with 0.5% BSA and 0.5% saponin. Cells were analyzed using a Cyan ADP flow cytometer (Beckman Coulter), Calibur (BD Bioscience), or Fortessa (BD Biosciences) and the Flowjo software package (Tree Star). For gating strategies, see Figure S7.

Antibodies and Plant Lectins

The following antibodies were used from eBioscience: anti-B220 (clone RA3-6B2), anti-CD11b (clone M1/70), anti-CD11c (clone N418), anti-Ly-6G/Gr-1 (clone RG6-8C5), anti-CD4 (Clone RM4-5), anti-CD11a (clone M17/4), anti-IFNγ (clone xM61.2), anti-VCAM-1 (clone 429), Fixable Viability Dye eFluor 780 and from Biolegend: anti-CD8α (clone 53-6.7), anti-VCAM-1 (clone 11-26c.2a). We produced and labeled the following antibodies in house: anti-MHC-II (clone M5/114), anti-CD169 (clones MOMA-1-488 or SER-4-488), isotype control (clone R7D4). Plant lectins were obtained from vector labs: Maackia Amurensis Lectin II (MALII) and Sambucus Nigra Lectin (SNA). Sytox blue nucleic acid stain (Invitrogen).

Immunofluorescence

Tissue sections were cut at 5–6 μM Mikrom HM 560 cryostat, fixed in 100% acetone, stained, and analyzed with a LEICA DM6000 or Leica TCS SP8 equipped with a pulsed white light laser and HyD hybrid detector equipped with temporal gating. LAS AF software was used for acquisition and ImageJ for image processing subsequent to data acquisition. Huygens professional deconvolution software was used for deconvolution.

Histocytometry

Spleen tissue was cryosectioned at 16 μM, and sections were rehydrated in 0.1 M Tris buffer for 30 min and blocked with blocking buffer (0.1 M Tris buffer, 0.02% Triton X-100, 1% normal mouse serum, anti-CD16/32 blocking Ab, 1% BSA) for 1 hr. Tissue sections were stained with directly labeled primary antibodies in blocking buffer for 16 hr at 4°C. After an extensive wash with 0.1 M Tris buffer, sections were mounted in Fluoromount-G (Thermo Fisher). Nuclei were counterstained with JOJO-1 Iodide (Thermo Fisher). Whole spleen cross-sections were acquired (voxel size y-x = 240 nm, z = 1 μm) on a Leica TCS SP8 confocal microscope with tunable pulsed white-light laser, 405 nm violet laser, and Leica HyD hybrid detectors. After acquisition, the tiled images were merged and compensated using the LAS X Merge and Channel Dye Separation module, respectively. Next, 3D stacked and compensated images were analyzed using histocytometry in Imaris 7.4 (Bitplane) and FlowJo as previously described (Gerner et al., 2012). In short, CD169 signal was used to segment $CD169^+$ macrophages by surface rendering and splitting individual cells using the Surface Module. The segmentation of dendritic cells was obtained by first creating a masking channel by selecting for $B220^-CD3^-MHCII^+CD11c^+$ voxels. The expression of CD4, CD8, MHCII, and CD11c on this masking channel was used as "true" DC expression of these markers. Next, a "dendritic cell" channel was created by combining $CD11c^+$ $MHCII^+$ voxels on the $B220^-CD3^-MHCII^+CD11c^+$ mask. This channel was used to segment and split individual dendritic cells using the Imaris Surface Module (Bitplane). Next, individual surfaces were exported to FlowJo and used for gating and figure representation.

Analysis of CD8 and CD4 T Cell Responses

Splenocytes from mice 7 days after i.v. immunization were re-stimulated *in vitro* for 5–6 hr with MHC class I restricted $OVA_{257–264}$ peptide (0.1 μg/mL), MVA-derived $B8R_{20–27}$ peptide, or VSV antigen p8 peptide or p52 peptide including GolgiPlug or Brefeldin A or for 18 hr with MHC class II restricted $OVA_{262–276}$ peptide (100 μg/mL) followed by 5 hr incubation with GolgiPlug (BD Biosciences). For tetramer stainings, splenocytes were incubated 45 min at 37°C with PE-labeled H2-K^b:SIINFEKL tetramers (generated at LUMC, Leiden, the Netherlands) in the presence of anti-CD8 Ab (clone 53-6,7). APC-labeled H-2K^b $B8R_{20–27}$ tetramers were provided by the NIH Tetramer Facility at Emory University.

Spleen Digestion

Spleens were cut and incubated in 1 mL per spleen of 2 WU/mL Liberase I (Roche Diagnostics GmbH, Mannheim, Germany) and 50 μg/mL DNase I (Roche) in medium without fetal calf serum (FCS) and β-mercaptoethanol with continuous stirring at 37°C for 15 min. EDTA was added to a 10 mM final concentration, and the cell suspension was incubated for an additional 5 min at 4°C. Red blood cells were lysed with ammonium-chloride-potassium lysis buffer. Cells were washed once and undigested material was removed by a 70–100 μM filter.

Ex Vivo Ag Presentation Assays

Mice were injected i.v. with 1 μg mAb-OVA plus 25 μg αCD40 and 25 μg poly (I:C). After 16 hr, DCs from 5–15 spleens were purified with anti-CD11c MACS microbeads (Miltenyi Biotec, Bergisch Gladbach, Germany) and co-cultured (2.5 × 10^5) with purified OT-I T cells (10^5) in triplicate in flat-bottomed 96-well plates. As a positive control, DCs were incubated with 1 μg/mL MHC class I $OVA_{257–264}$ peptide for 1 hr and washed three times. After 48 hr, plates were pulsed with 1 μCi/well of [^{3}H]-thymidine. After an additional 16 hr, [^{3}H]-thymidine incorporation was measured on a Wallac-LKB Betaplate 1205 liquid scintillation counter. Data were summarized by the mean and SEM.

In Vivo Ag Transfer Assays

Mice were immunized i.v. with 1 μg mAb-Alexa488 or mAb-biotin in the presence or absence of 25 μg poly(I:C) and 25 μg αCD40 Ab 1C10. Ten minutes or 2 hr after injection, mice were sacrificed and spleens were digested for fluorescence-activated cell sorting (FACS) analysis or frozen for immunofluorescence analysis.

Imaging Flow Cytometry

After digestion, splenocytes from three mice were pooled, stained for surface markers, and fixed in 2% paraformaldehyde. Cells were analyzed using the ImageStreamX (Merck Millipore) imaging flow cytometer. Internalization scores were calculated as previously described (García-Vallejo et al., 2014). In short, a mask was designed based on the bright-field morphology image that was eroded until the membrane was left out of the mask. Alexa488 signal within this mask was defined as intracellular, while Alexa488 signal outside was defined as membrane-associated. The internalization score was calculated using the internalization feature provided in Ideas v6.0 software (Merck Millipore). Scores below 0 indicate that the majority of the signal is membrane-associated, while scores above 0 indicate that the majority of the signal is intracellular.

Lectin and CD169 Binding Assays and Neuraminidase Treatment

Biotinylated plant lectins from Maackia amurensis Lectin-II (MAL-II) and Sambucus nigra (SNA) were incubated with DCs for 30 min at 37°C in TSM buffer (20 mM Tris [pH 7.4], 150 mM NaCl, 1 mM $CaCl_2$, and 2 mM $MgCl_2$) with 0.5% BSA (Fluka Biochemika), followed by additional stainings at 4°C. For CD169-Fc binding assays, DCs were incubated with pre-complexed CD169-Fc or CD169-Fc-R97A (1–10 μg/mL) with goat-anti-Human-Fc-Alexa488 (0.5 μg/mL, Invitrogen) in TSM buffer with 1% BSA (Fluka Biochemika) for 45 min at room temperature or 1 hr on ice and analyzed by flow cytometry. For neuraminidase treatment cells were incubated in DMEM without FCS with 1:60 sialidase (Sigma) for 1 hr at 37°C and mixed gently every 15 min.

Statistical Analysis

Statistical significance was tested using GraphPad Prism by performing a two-tailed student-t test, ANOVA with Bonferroni's correction, or a Kruskal-Wallis test with Bonferroni's correction (*$p < 0.05$, **$p < 0.01$, ***$p < 0.001$, ****$p < 0.0001$; n.s., non-significant). N represents the number of animals used in the experiment.

SUPPLEMENTAL INFORMATION

Supplemental Information includes Supplemental Experimental Procedures and seven figures and can be found with this article online at https://doi.org/10.1016/j.celrep.2018.01.021.

ACKNOWLEDGMENTS

We thank J.J. Koning for help on IMARIS and J.P. Middelberg, C. Prins, and R. van der Laan for animal care. We acknowledge the NIH Tetramer Core Facility (contract HHSN272201300006C) for MHC-I tetramers. We thank Mariano Esteban for the MVA-GFP strain. Work in the D.S. laboratory is funded by the CNIC; grant SAF2016-79040-R from the Spanish Ministry of Economy, Industry and Competitiveness (MINECO), Agencia Estatal de Investigación and FEDER (European fund for Regional Development); Foundation Acteria; and the European Commission (635122-PROCROP H2020) and the European Research Council (ERC-2016-Consolidator Grant 725091). This work was supported by grants from the Dutch Cancer Society (VU2009-4504 and VU2013-5940) and by VUmc CCA (2015-5-22 to J.M.M.d.H.). S.I. is funded by grant SAF2015-74561-JIN.

AUTHOR CONTRIBUTIONS

Experimental design by D.v.D., H.V., M.R.B., D.S., K.S.L., L.B.C., P.R.C., and J.M.M.d.H. Experiments were conducted by D.v.D., H.V., S.I., E.G.F.B., L.H., K.O., S.T.T.S., K.S.L., and M.R.B. H.K. and K.L.F. synthesized conjugates and tetramers. Data analysis by D.v.D., H.V., S.T.T.S., S.I., K.S.L., M.R.B., and J.J.G.-V. The manuscript written by J.M.M.d.H. and D.v.D. and edited by all authors.

DECLARATION OF INTERESTS

The authors declare no competing interests.

Received: August 1, 2017
Revised: December 12, 2017
Accepted: January 8, 2018
Published: February 6, 2018

REFERENCES

Ahrens, S., Zelenay, S., Sancho, D., Hanč, P., Kjær, S., Feest, C., Fletcher, G., Durkin, C., Postigo, A., Skehel, M., et al. (2012). F-actin is an evolutionarily conserved damage-associated molecular pattern recognized by DNGR-1, a receptor for dead cells. Immunity *36*, 635–645.

Aichele, P., Zinke, J., Grode, L., Schwendener, R.A., Kaufmann, S.H., and Seiler, P. (2003). Macrophages of the splenic marginal zone are essential for trapping of blood-borne particulate antigen but dispensable for induction of specific T cell responses. J. Immunol. *171*, 1148–1155.

Asano, K., Nabeyama, A., Miyake, Y., Qiu, C.H., Kurita, A., Tomura, M., Kanagawa, O., Fujii, S., and Tanaka, M. (2011). CD169-positive macrophages dominate antitumor immunity by crosspresenting dead cell-associated antigens. Immunity *34*, 85–95.

Backer, R., Schwandt, T., Greuter, M., Oosting, M., Jüngerkes, F., Tüting, T., Boon, L., O'Toole, T., Kraal, G., Limmer, A., and den Haan, J.M. (2010). Effective collaboration between marginal metallophilic macrophages and CD8+ dendritic cells in the generation of cytotoxic T cells. Proc. Natl. Acad. Sci. USA *107*, 216–221.

Barral, P., Polzella, P., Bruckbauer, A., van Rooijen, N., Besra, G.S., Cerundolo, V., and Batista, F.D. (2010). CD169(+) macrophages present lipid antigens to mediate early activation of iNKT cells in lymph nodes. Nat. Immunol. *11*, 303–312.

Berney, C., Herren, S., Power, C.A., Gordon, S., Martinez-Pomares, L., and Kosco-Vilbois, M.H. (1999). A member of the dendritic cell family that enters B cell follicles and stimulates primary antibody responses identified by a mannose receptor fusion protein. J. Exp. Med. *190*, 851–860.

Bernhard, C.A., Ried, C., Kochanek, S., and Brocker, T. (2015). CD169+ macrophages are sufficient for priming of CTLs with specificities left out by cross-priming dendritic cells. Proc. Natl. Acad. Sci. USA *112*, 5461–5466.

Carrasco, Y.R., and Batista, F.D. (2007). B cells acquire particulate antigen in a macrophage-rich area at the boundary between the follicle and the subcapsular sinus of the lymph node. Immunity *27*, 160–171.

Ciavarra, R.P., Buhrer, K., Van Rooijen, N., and Tedeschi, B. (1997). T cell priming against vesicular stomatitis virus analyzed in situ: red pulp macrophages, but neither marginal metallophilic nor marginal zone macrophages, are required for priming CD4+ and CD8+ T cells. J. Immunol. *158*, 1749–1755.

Crocker, P.R., and Gordon, S. (1989). Mouse macrophage hemagglutinin (sheep erythrocyte receptor) with specificity for sialylated glycoconjugates characterized by a monoclonal antibody. J. Exp. Med. *169*, 1333–1346.

Crocker, P.R., Mucklow, S., Bouckson, V., McWilliam, A., Willis, A.C., Gordon, S., Milon, G., Kelm, S., and Bradfield, P. (1994). Sialoadhesin, a macrophage sialic acid binding receptor for haemopoietic cells with 17 immunoglobulin-like domains. EMBO J. *13*, 4490–4503.

Crocker, P.R., Freeman, S., Gordon, S., and Kelm, S. (1995). Sialoadhesin binds preferentially to cells of the granulocytic lineage. J. Clin. Invest. *95*, 635–643.

Delputte, P.L., Van Breedam, W., Delrue, I., Oetke, C., Crocker, P.R., and Nauwynck, H.J. (2007). Porcine arterivirus attachment to the macrophage-specific receptor sialoadhesin is dependent on the sialic acid-binding activity of the N-terminal immunoglobulin domain of sialoadhesin. J. Virol. *81*, 9546–9550.

den Haan, J.M., and Bevan, M.J. (2002). Constitutive versus activation-dependent cross-presentation of immune complexes by CD8(+) and CD8(-) dendritic cells in vivo. J. Exp. Med. *196*, 817–827.

den Haan, J.M., Lehar, S.M., and Bevan, M.J. (2000). CD8(+) but not CD8(-) dendritic cells cross-prime cytotoxic T cells in vivo. J. Exp. Med. *192*, 1685–1696.

Di Pilato, M., Mejías-Pérez, E., Gómez, C.E., Perdiguero, B., Sorzano, C.O., and Esteban, M. (2013). New vaccinia virus promoter as a potential candidate for future vaccines. J. Gen. Virol. *94*, 2771–2776.

Dudziak, D., Kamphorst, A.O., Heidkamp, G.F., Buchholz, V.R., Trumpfheller, C., Yamazaki, S., Cheong, C., Liu, K., Lee, H.W., Park, C.G., et al. (2007). Differential antigen processing by dendritic cell subsets in vivo. Science *315*, 107–111.

Eickhoff, S., Brewitz, A., Gerner, M.Y., Klauschen, F., Komander, K., Hemmi, H., Garbi, N., Kaisho, T., Germain, R.N., and Kastenmüller, W. (2015). Robust anti-viral immunity requires multiple distinct T cell-dendritic cell interactions. Cell *162*, 1322–1337.

Eloranta, M.L., and Alm, G.V. (1999). Splenic marginal metallophilic macrophages and marginal zone macrophages are the major interferon-alpha/beta producers in mice upon intravenous challenge with herpes simplex virus. Scand. J. Immunol. *49*, 391–394.

Erikson, E., Wratil, P.R., Frank, M., Ambiel, I., Pahnke, K., Pino, M., Azadi, P., Izquierdo-Useros, N., Martinez-Picado, J., Meier, C., et al. (2015). Mouse Siglec-1 mediates trans-infection of surface-bound murine leukemia virus in a sialic acid N-acyl side chain-dependent manner. J. Biol. Chem. *290*, 27345–27359.

García-Vallejo, J.J., Ilarregui, J.M., Kalay, H., Chamorro, S., Koning, N., Unger, W.W., Ambrosini, M., Montserrat, V., Fernandes, R.J., Bruijns, S.C., et al. (2014). CNS myelin induces regulatory functions of DC-SIGN-expressing, antigen-presenting cells via cognate interaction with MOG. J. Exp. Med. *211*, 1465–1483.

Gaya, M., Castello, A., Montaner, B., Rogers, N., Reis e Sousa, C., Bruckbauer, A., and Batista, F.D. (2015). Host response. Inflammation-induced disruption of SCS macrophages impairs B cell responses to secondary infection. Science *347*, 667–672.

Gerner, M.Y., Kastenmuller, W., Ifrim, I., Kabat, J., and Germain, R.N. (2012). Histo-cytometry: a method for highly multiplex quantitative tissue imaging analysis applied to dendritic cell subset microanatomy in lymph nodes. Immunity *37*, 364–376.

Gupta, P., Lai, S.M., Sheng, J., Tetlak, P., Balachander, A., Claser, C., Renia, L., Karjalainen, K., and Ruedl, C. (2016). Tissue-resident CD169(+) macrophages form a crucial front line against plasmodium infection. Cell Rep. *16*, 1749–1761.

Habbeddine, M., Verthuy, C., Rastoin, O., Chasson, L., Bebien, M., Bajenoff, M., Adriouch, S., den Haan, J.M.M., Penninger, J.M., and Lawrence, T.

(2017). Receptor activator of NF-κB orchestrates activation of antiviral memory CD8 T cells in the spleen marginal zone. Cell Rep. *21*, 2515–2527.

Hildner, K., Edelson, B.T., Purtha, W.E., Diamond, M., Matsushita, H., Kohyama, M., Calderon, B., Schraml, B.U., Unanue, E.R., Diamond, M.S., et al. (2008). Batf3 deficiency reveals a critical role for CD8alpha+ dendritic cells in cytotoxic T cell immunity. Science *322*, 1097–1100.

Honke, N., Shaabani, N., Cadeddu, G., Sorg, U.R., Zhang, D.E., Trilling, M., Klingel, K., Sauter, M., Kandolf, R., Gailus, N., et al. (2011). Enforced viral replication activates adaptive immunity and is essential for the control of a cytopathic virus. Nat. Immunol. *13*, 51–57.

Hor, J.L., Whitney, P.G., Zaid, A., Brooks, A.G., Heath, W.R., and Mueller, S.N. (2015). Spatiotemporally distinct interactions with dendritic cell subsets facilitates CD4+ and CD8+ T cell activation to localized viral infection. Immunity *43*, 554–565.

Iannacone, M., Moseman, E.A., Tonti, E., Bosurgi, L., Junt, T., Henrickson, S.E., Whelan, S.P., Guidotti, L.G., and von Andrian, U.H. (2010). Subcapsular sinus macrophages prevent CNS invasion on peripheral infection with a neurotropic virus. Nature *465*, 1079–1083.

Iborra, S., Izquierdo, H.M., Martínez-López, M., Blanco-Menéndez, N., Reis e Sousa, C., and Sancho, D. (2012). The DC receptor DNGR-1 mediates cross-priming of CTLs during vaccinia virus infection in mice. J. Clin. Invest. *122*, 1628–1643.

Iborra, S., Martínez-López, M., Khouili, S.C., Enamorado, M., Cueto, F.J., Conde-Garrosa, R., Del Fresno, C., and Sancho, D. (2016). Optimal generation of tissue-resident but not circulating memory T cells during viral infection requires crosspriming by DNGR-1+ dendritic cells. Immunity *45*, 847–860.

Iyoda, T., Shimoyama, S., Liu, K., Omatsu, Y., Akiyama, Y., Maeda, Y., Takahara, K., Steinman, R.M., and Inaba, K. (2002). The CD8+ dendritic cell subset selectively endocytoses dying cells in culture and in vivo. J. Exp. Med. *195*, 1289–1302.

Jung, S., Unutmaz, D., Wong, P., Sano, G., De los Santos, K., Sparwasser, T., Wu, S., Vuthoori, S., Ko, K., Zavala, F., et al. (2002). In vivo depletion of CD11c+ dendritic cells abrogates priming of CD8+ T cells by exogenous cell-associated antigens. Immunity *17*, 211–220.

Junt, T., Moseman, E.A., Iannacone, M., Massberg, S., Lang, P.A., Boes, M., Fink, K., Henrickson, S.E., Shayakhmetov, D.M., Di Paolo, N.C., et al. (2007). Subcapsular sinus macrophages in lymph nodes clear lymph-borne viruses and present them to antiviral B cells. Nature *450*, 110–114.

Kastenmüller, W., Torabi-Parizi, P., Subramanian, N., Lämmermann, T., and Germain, R.N. (2012). A spatially-organized multicellular innate immune response in lymph nodes limits systemic pathogen spread. Cell *150*, 1235–1248.

Kawasaki, N., Vela, J.L., Nycholat, C.M., Rademacher, C., Khurana, A., van Rooijen, N., Crocker, P.R., Kronenberg, M., and Paulson, J.C. (2013). Targeted delivery of lipid antigen to macrophages via the CD169/sialoadhesin endocytic pathway induces robust invariant natural killer T cell activation. Proc. Natl. Acad. Sci. USA *110*, 7826–7831.

Klaas, M., Oetke, C., Lewis, L.E., Erwig, L.P., Heikema, A.P., Easton, A., Willison, H.J., and Crocker, P.R. (2012). Sialoadhesin promotes rapid proinflammatory and type I IFN responses to a sialylated pathogen, Campylobacter jejuni. J. Immunol. *189*, 2414–2422.

Macauley, M.S., Crocker, P.R., and Paulson, J.C. (2014). Siglec-mediated regulation of immune cell function in disease. Nat. Rev. Immunol. *14*, 653–666.

Martinez-Pomares, L., and Gordon, S. (2012). CD169+ macrophages at the crossroads of antigen presentation. Trends Immunol. *33*, 66–70.

Phan, T.G., Grigorova, I., Okada, T., and Cyster, J.G. (2007). Subcapsular encounter and complement-dependent transport of immune complexes by lymph node B cells. Nat. Immunol. *8*, 992–1000.

Phan, T.G., Green, J.A., Gray, E.E., Xu, Y., and Cyster, J.G. (2009). Immune complex relay by subcapsular sinus macrophages and noncognate B cells drives antibody affinity maturation. Nat. Immunol. *10*, 786–793.

Puryear, W.B., Akiyama, H., Geer, S.D., Ramirez, N.P., Yu, X., Reinhard, B.M., and Gummuluru, S. (2013). Interferon-inducible mechanism of dendritic cell-mediated HIV-1 dissemination is dependent on Siglec-1/CD169. PLoS Pathog. *9*, e1003291.

Sagoo, P., Garcia, Z., Breart, B., Lemaître, F., Michonneau, D., Albert, M.L., Levy, Y., and Bousso, P. (2016). In vivo imaging of inflammasome activation reveals a subcapsular macrophage burst response that mobilizes innate and adaptive immunity. Nat. Med. *22*, 64–71.

Sancho, D., Joffre, O.P., Keller, A.M., Rogers, N.C., Martínez, D., Hernanz-Falcón, P., Rosewell, I., and Reis e Sousa, C. (2009). Identification of a dendritic cell receptor that couples sensing of necrosis to immunity. Nature *458*, 899–903.

Schulz, O., and Reis e Sousa, C. (2002). Cross-presentation of cell-associated antigens by CD8alpha+ dendritic cells is attributable to their ability to internalize dead cells. Immunology *107*, 183–189.

Segura, E., and Amigorena, S. (2015). Cross-presentation in mouse and human dendritic cells. Adv. Immunol. *127*, 1–31.

Segura, E., Kapp, E., Gupta, N., Wong, J., Lim, J., Ji, H., Heath, W.R., Simpson, R., and Villadangos, J.A. (2010). Differential expression of pathogen-recognition molecules between dendritic cell subsets revealed by plasma membrane proteomic analysis. Mol. Immunol. *47*, 1765–1773.

Seiler, P., Aichele, P., Odermatt, B., Hengartner, H., Zinkernagel, R.M., and Schwendener, R.A. (1997). Crucial role of marginal zone macrophages and marginal zone metallophils in the clearance of lymphocytic choriomeningitis virus infection. Eur. J. Immunol. *27*, 2626–2633.

Sewald, X., Ladinsky, M.S., Uchil, P.D., Beloor, J., Pi, R., Herrmann, C., Motamedi, N., Murooka, T.T., Brehm, M.A., Greiner, D.L., et al. (2015). Retroviruses use CD169-mediated trans-infection of permissive lymphocytes to establish infection. Science *350*, 563–567.

Silvin, A., Yu, C., Lahaye, X., Imperatore, F., Brault, J., Cardinaud, S., Becker, C., Kwan, W., Conrad, C., Maurin, M., et al. (2017). Constitutive resistance to viral infection in human CD141+ dendritic cells. Sci. Immunol. *2*, eaai8071.

van den Berg, T.K., Brevé, J.J., Damoiseaux, J.G., Döpp, E.A., Kelm, S., Crocker, P.R., Dijkstra, C.D., and Kraal, G. (1992). Sialoadhesin on macrophages: its identification as a lymphocyte adhesion molecule. J. Exp. Med. *176*, 647–655.

van Montfoort, N., de Jong, J.M., Schuurhuis, D.H., van der Voort, E.I., Camps, M.G., Huizinga, T.W., van Kooten, C., Daha, M.R., Verbeek, J.S., Ossendorp, F., and Toes, R.E. (2007). A novel role of complement factor C1q in augmenting the presentation of antigen captured in immune complexes to CD8+ T lymphocytes. J. Immunol. *178*, 7581–7586.

Veninga, H., Borg, E.G., Vreeman, K., Taylor, P.R., Kalay, H., van Kooyk, Y., Kraal, G., Martinez-Pomares, L., and den Haan, J.M. (2015). Antigen targeting reveals splenic CD169+ macrophages as promoters of germinal center B-cell responses. Eur. J. Immunol. *45*, 747–757.

Vinson, M., van der Merwe, P.A., Kelm, S., May, A., Jones, E.Y., and Crocker, P.R. (1996). Characterization of the sialic acid-binding site in sialoadhesin by site-directed mutagenesis. J. Biol. Chem. *271*, 9267–9272.

Winkelmann, E.R., Widman, D.G., Xia, J., Johnson, A.J., van Rooijen, N., Mason, P.W., Bourne, N., and Milligan, G.N. (2014). Subcapsular sinus macrophages limit dissemination of West Nile virus particles after inoculation but are not essential for the development of West Nile virus-specific T cell responses. Virology *450-451*, 278–289.

Zelenay, S., Keller, A.M., Whitney, P.G., Schraml, B.U., Deddouche, S., Rogers, N.C., Schulz, O., Sancho, D., and Reis e Sousa, C. (2012). The dendritic cell receptor DNGR-1 controls endocytic handling of necrotic cell antigens to favor cross-priming of CTLs in virus-infected mice. J. Clin. Invest. *122*, 1615–1627.

Zhang, Y., Roth, T.L., Gray, E.E., Chen, H., Rodda, L.B., Liang, Y., Ventura, P., Villeda, S., Crocker, P.R., and Cyster, J.G. (2016). Migratory and adhesive cues controlling innate-like lymphocyte surveillance of the pathogen-exposed surface of the lymph node. eLife *5*, e18156.